Terahertz generation from graphite

Gopakumar Ramakrishnan*, Reshmi Chakkittakandy, and Paul C. M. Planken

Optics Research Group, Department of Imaging Science and Technology, Faculty of Applied Sciences
Delft University of Technology, Lorentzweg 1, 2628 CJ, Delft, The Netherlands
*G.Ramakrishnan@tudelft.nl

Abstract: Generation of subpicosecond terahertz pulses is observed when graphite surfaces are illuminated with femtosecond near-infrared laser pulses. The nonlinear optical generation of THz pulses from graphite is unexpected since, in principle, the material possesses a centre of inversion symmetry. Experiments with highly oriented pyrolytic graphite crystals suggest that the THz radiation is generated by a transient photocurrent in a direction normal to the graphene planes, along the c-axis of the crystal. This is supported by magnetic-field induced changes in the THz electric-field polarization, and consequently, the direction of the photocurrent. We show that other forms of graphite, such as a pencil drawing on paper, are also capable of emitting THz pulses.

©2009 Optical Society of America

OCIS codes: (300.6495) Spectroscopy, terahertz; (300.6270) Spectroscopy, far infrared; (260.7120) Ultrafast phenomena; (160.4760) Optical properties

References and links

1. G. Brumfiel, "Graphene gets ready for the big time," Nature **458**(7237), 390–391 (2009).
2. K. S. Krishnan, and N. Ganguly, "Large anisotropy of the electrical conductivity of graphite," Nature **144**(3650), 667 (1939).
3. M. Zanini, D. Grubisic, and J. E. Fischer, "Optical anisotropy of highly oriented pyrolytic graphite," Phys. Status Solidi, B Basic Res. **90**(1), 151–156 (1978).
4. B. T. Kelly, "Physics of graphite," Applied Science Publishers Ltd., Essex (1981).
5. W. N. Reynolds, "Physical properties of graphite," Elsevier Publishing Co. Ltd., Amsterdam (1968).
6. M. Breusing, C. Ropers, and T. Elsaesser, "Ultrafast carrier dynamics in graphite," Phys. Rev. Lett. **102**(8), 086809 (2009).
7. K. Seibert, G. C. Cho, W. Kütt, H. Kurz, D. H. Reitze, J. I. Dadap, H. Ahn, M. C. Downer, and A. M. Malvezzi, "Femtosecond carrier dynamics in graphite," Phys. Rev. B **42**(5), 2842–2851 (1990).
8. G. M. Mikheev, R. G. Zonov, A. N. Obraztov, and Yu. P. Svirko, "Giant optical rectification effect in nanocarbon films," Appl. Phys. Lett. **84**(24), 4854–4856 (2004).
9. R. W. Newson, J.-M. Ménard, C. Sames, M. Betz, and H. M. van Driel, "Coherently controlled ballistic charge currents injected in single-walled carbon nanotubes and graphite," Nano Lett. **8**(6), 1586–1589 (2008).
10. N. C. J. van der Valk, W. Th. Wenckebach, and P. C. M. Planken, "Full mathematical description of electro-optic detection in optically isotropic crystals," J. Opt. Soc. Am. B **21**(3), 622–631 (2004).
11. G. Zhao, R. N. Schouten, N. van der Valk, W. Th. Wenckebach, and P. C. M. Planken, "Design and performance of a THz emission and detection setup based on a semi-insulating GaAs emitter," Rev. Sci. Instrum. **73**(4), 1715–1719 (2002).
12. http://www.optigraph.fta-berlin.de/
13. H. Legall, H. Stiel, A. Antonov, I. Grigorieva, V. Arkadiev, and A. Bjeoumikhov, "A new generation of X-ray optics based on pyrolytic graphite," in Proceedings of 28th International Free Electron Laser conference, (BESSY, Berlin, Germany, 2006) pp. 798–801.
14. N. C. J. van der Valk, P. C. M. Planken, A. N. Buijserd, and H. J. Bakker, "Influence of pump wavelength and crystal length on the phase matching of optical rectification," J. Opt. Soc. Am. B **22**(8), 1714–1718 (2005).
15. X.-C. Zhang, Y. Jin, L. E. Kingsley, and M. Weiner, "Influence of electric and magnetic fields on THz radiation," Appl. Phys. Lett. **62**(20), 2477–2479 (1993).
16. N. Sarukura, H. Ohtake, S. Izumida, and Z. Liu, "High average-power THz radiation from femtosecond laser-irradiated InAs in a magnetic field and its elliptical polarization characteristics," J. Appl. Phys. **84**(1), 654–656 (1998).
17. J. Shan, C. Weiss, R. Wallenstein, R. Beigang, and T. F. Heinz, "Origin of magnetic field enhancement in the generation of terahertz radiation from semiconductor surfaces," Opt. Lett. **26**(11), 849–851 (2001).
18. M. B. Johnston, D. M. Whittaker, A. Corchia, A. G. Davies, and E. H. Linfield, "Theory of magnetic-field enhancement of surface-field terahertz emission," J. Appl. Phys. **91**, 2104–2106 (2002).
19. A. D. Modestov, J. Gun, and O. Lev, "Graphite photochemistry 2. Photochemical studies of highly oriented pyrolitic graphite," J. Electroanal. Chem. **476**(2), 118–131 (1999).

20. J.-P. Randin, and E. Yeager, "Differential capacitance studies on the basal plane of stress-annealed pyrolytic graphite," J. Electroanal. Chem. **36**(2), 257–276 (1972).
21. H. Dember, "Photoelectromotive force in cuprous oxide crystals," Phys. Z. **32**, 554–556 (1931).
22. M. B. Johnston, D. M. Whittaker, A. Corchia, A. G. Davies, and E. H. Linfield, "Simulation of terahertz generation at semiconductor surfaces," Phys. Rev. B **65**(16), 165301 (2002).
23. S. R. Snyder, T. Foecke, H. S. White, and W. W. Gerberich, "Imaging of stacking faults in highly oriented pyrolytic graphite using scanning tunneling microscopy," J. Mater. Res. **7**(2), 341–344 (1992).
24. Y. Lu, M. Muñoz, C. S. Steplecaru, C. Hao, M. Bai, N. Garcia, K. Schindler, and P. Esquinazi, "Electrostatic force microscopy on oriented graphite surfaces: coexistence of insulating and conducting behaviors," Phys. Rev. Lett. **97**(7), 076805 (2006).
25. S. Banerjee, M. Sardar, N. Gayathri, A. K. Thyagi, and B. Raj, "Conductivity landscape of highly oriented pyrolytic graphite surfaces containing ribbons and edges," Phys. Rev. B **72**(7), 075418 (2005).
26. G. D. Metcalfe, H. Shen, M. Wraback, A. Hirai, F. Wu, and J. S. Speck, "Enhanced terahertz radiation from high stacking fault density nonpolar GaN," Appl. Phys. Lett. **92**(24), 241106 (2008).
27. E. Abraham, A. Younus, A. El Fatimy, J. C. Delagnes, E. Nguéma, and P. Mounaix, "Broadband terahertz imaging of documents written with lead pencils," Opt. Commun. **282**(15), 3104–3107 (2009).

1. Introduction

There has been increased interest recently in graphite and related systems, such as graphene and carbon nanotubes, because of their potential application in carbon-based electronics [1]. Graphite is an allotrope of carbon, classified as a semimetal. Structurally, graphite crystals consist of stacks of identical atomic planes of carbon. Within each single plane, carbon atoms interact much more strongly than with those from the adjacent planes, and form covalent bonds in a honeycomb structure possessing hexagonal symmetry. Such a two dimensional single-atom thick plane is called graphene. Different graphene planes in graphite are attached to each other by weak van der Waals forces. Thermal, electrical and optical properties of graphite parallel and perpendicular to these graphene layers are known to be different [2,3]. This peculiar structure gives graphite unique qualities which are widely made use of in its different applications [4,5]. To this end, extensive studies have been performed on the transport properties and ultrafast carrier dynamics in graphite [6,7]. A recent report discusses the observation of second-order nonlinear optical rectification of nanosecond laser pulses by nano-graphite films, proposing that magnetic dipoles or electric quadrupoles are responsible [8]. This suggests the possibility of using graphite surfaces and related materials as sources of electromagnetic radiation in the THz region. In principle, graphite is a centrosymmetric system, which does not allow electric dipole second-order nonlinear processes from the bulk of the crystal. Another report shows the generation of photocurrents in carbon nanotubes and graphite using a *third-order* nonlinear optical process [9]. In that experiment, laser pulses with a central wavelength of 1400 nm and its second harmonic are focused onto a graphite surface to create the photocurrent. The magnitude and sign of the photocurrent are determined by the phase difference between the two optical beams. This transient photocurrent is detected via the emitted THz radiation. In principle, third-order nonlinear processes are allowed in all media, whether they possess inversion symmetry or not. So far, however, no report has been published on the emission of THz radiation from graphite using a *second-order* nonlinear optical process.

Here we report on the generation of THz pulses from highly oriented pyrolytic graphite (HOPG) samples illuminated with femtosecond laser pulses. We observe the emission of THz radiation from all faces of the rectangular cuboid crystal when they are illuminated at an angle of incidence of 45°. However, when the incident laser beam propagation direction is perpendicular to the graphene planes, little or no THz emission is observed in the back-reflected direction. Surprisingly, the dependence of the THz electric-field amplitude on the laser pump power indicates that the phenomenon is a *second-order* nonlinear optical process, even though crystalline bulk graphite is a centrosymmetric system. We suggest that the THz electric-field is generated by transient photo-induced charge movement along the normal to the graphene planes, in the direction of the c-axis of the crystal. The involvement of charge movement is confirmed by in-plane magnetic-field induced changes in the generated THz electric-field. Interestingly, other forms of graphite, such as pencil lead and even a pencil

drawing on paper, also emit coherent THz pulses when illuminated with femtosecond laser pulses.
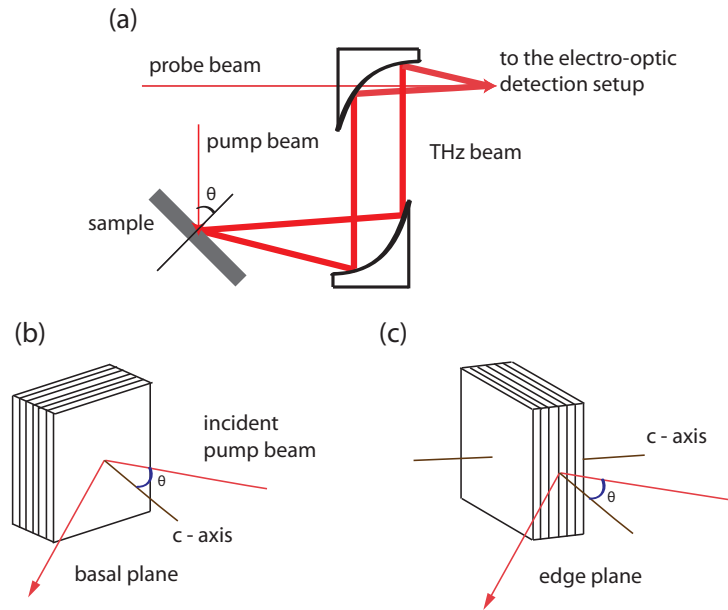
2. Experimental

Fig. 1. (a) The schematic of the experimental setup used for the experiments. The angle of incidence of the pump beam is shown as θ. (b) Schematic representation of the illumination of the basal plane surface of the HOPG crystal, showing the orientation of the graphene planes. (c) Schematic representation of the illumination of the edge plane surface.

The experimental setup is shown in Fig. 1(a). The laser source used is a Ti: Sapphire oscillator (Scientific XL, Femtolasers) generating pulses of 50 fs duration, centered at a wavelength of 800 nm with a repetition rate of 11 MHz. The average power output from the laser is 800 mW. The output from the oscillator is split into two arms by a 20/80 beam splitter. The 80% part (pump) is used as the pump beam, and the 20% part (probe) as the sampling beam. The pump beam is sent to an in-plane retro-reflector mounted on a loudspeaker oscillating at 50 Hz, and is then focused onto the sample surface. We performed experiments with two different angles of incidence of the illuminating beam; 0° (normal incidence) and 45°, on different faces of the HOPG crystal as shown in Fig. 1(b) and 1(c). In all cases, the THz radiation generated from the graphite sample is collected in the reflected direction using off-axis parabolic mirrors and focused onto an electro-optic detection crystal (ZnTe (110) or GaP (110)) [10]. The synchronized, co-propagating, sampling pulse is also focused onto the detection crystal. The THz electric-field elliptically polarizes the probe beam to an extent proportional to the instantaneous THz electric-field value. The probe beam then propagates towards a differential detection setup consisting of a quarter wave plate, a Wollaston prism and a differential detector. This setup measures the ellipticity of the beam and thus the instantaneous THz electric-field strength. Since the optical delay between the pump pulse (and thus the THz pulse) and the sampling pulse oscillates at 50 Hz, a full 25 ps long THz electric-field time-trace is obtained every 20 ms [11].

HOPG crystals were purchased from Optigraph GmbH, Berlin, and were used in the experiments with freshly cleaved surfaces, mostly without further processing [12]. The quality of HOPG crystals is usually expressed in terms of the consistency in the alignment of the micro-crystallites in them. The angular spread in the orientation of the c-axes of the micro-crystallites is called the mosaic spread [13]. HOPG crystals usually have a mosaic spread of < 1°, and in our experiments we used crystals of mosaic spread 0.8° as well as 0.4°. The face of

the crystal which ideally ends with a graphene plane with the c-axis normal to the surface, is called the basal plane surface and the crystal faces perpendicular to it are called the edge plane surfaces. Both the basal plane surfaces and the edge plane surfaces of the crystal were used in our experiments for the generation of THz radiation.

3. Results and discussion

3.1 Basal-plane surface illumination

Figure 2(a) shows the temporal waveform of the electric-field generated from the basal plane surface of an HOPG crystal, electro-optically detected in a nitrogen purged environment using a 500 µm thick ZnTe (110) crystal. The angle of incidence of the pump beam was 45°. The waveform consists of a nearly single-cycle pulse followed by a rapidly oscillating decaying tail. The rapidly oscillating tail is due to the phase matching in the detection crystal where the phase velocity of the THz radiation is different from the group velocity of the probe radiation [14]. The polarization of the emitted THz pulses was checked with a wire grid polarizer and was found to be in the plane of incidence, irrespective of the polarization of the pump beam. Little or no horizontally and vertically polarized THz electric-field components are detected in the back-reflected direction, when the angle of incidence of the pump beam is 0°. All of this indicates that the emission is predominantly due to a possible transient charge movement along the surface normal when the basal plane is illuminated. Based on this, the weak electric-field emission observed at 0° pump incidence can be attributed to the misalignments of the micro-crystallites, which could give rise to a small current component parallel to the sample surface.
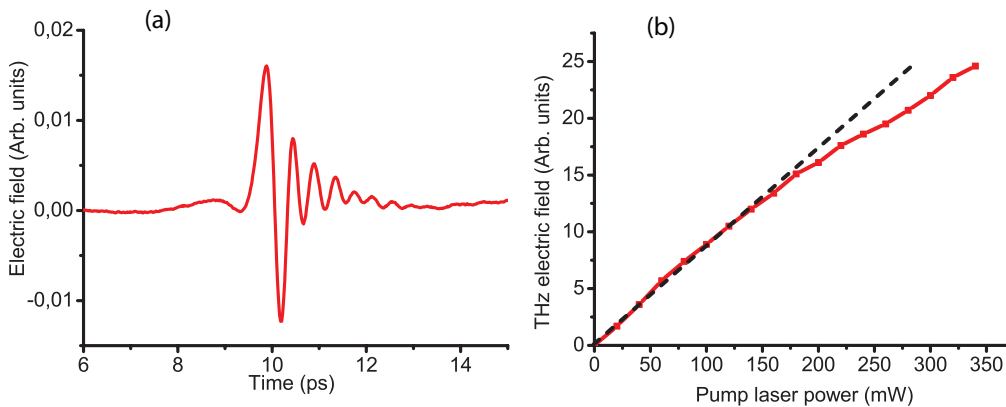

Fig. 2. (a) THz electric-field detected using a 500 µm thick ZnTe (110) crystal. (b) The dependence of the generated THz electric-field on the incident pump power. The dashed black line is a linear fit to the data at low pump power.

At 45° illumination, the THz electric-field generated from the basal plane surface of the crystal does not depend on the azimuthal orientation of the crystal, which suggests the absence of any preferential direction of charge movement within the basal plane. In principle, there are three equivalent directions in the basal plane owing to the symmetry of arrangement of carbon atoms [4]. However, we do not observe any effect of this in the azimuthal angle dependence.

Scotch tape was used to remove layers of graphene stacks from the basal plane and fresh surfaces were tested for their ability to generate THz pulses during illumination with femtosecond laser pulses. The THz pulses generated from different freshly cleaved surfaces all look similar in shape and amplitude. The polarity of the generated THz electric-field is the same for the two opposite faces of the crystal. Generation of THz radiation at the basal plane of the crystal is thus likely a surface phenomenon, which is identical for all the HOPG basal plane surfaces tested.

The amplitude of the generated electric field is about 5% of that generated from an unbiased semi-insulating GaAs (100) surface at pump intensities below about 3 W/cm^2, and is

opposite in polarity. This increases to about 11% at higher pump powers, presumably due to the difference in pump power saturation between the two materials. The dependence of the amplitude of the generated THz electric field on the pump power is shown in Fig. 2(b). At low pump powers the dependence is linear, which is indicative of a second-order nonlinear process. At higher powers, the THz generation increases sub-linearly, indicating the onset of saturation. Graphite, in principle, is a material which possesses a centre of inversion symmetry, which prohibits $\chi^{(2)}$ processes from the bulk of the crystal [8]. Based on the fact that graphite is more or less opaque to the pump beam, the generation of THz radiation near the surface must be localized to a thin layer consisting of multiple graphene planes within the penetration depth of the pump beam.
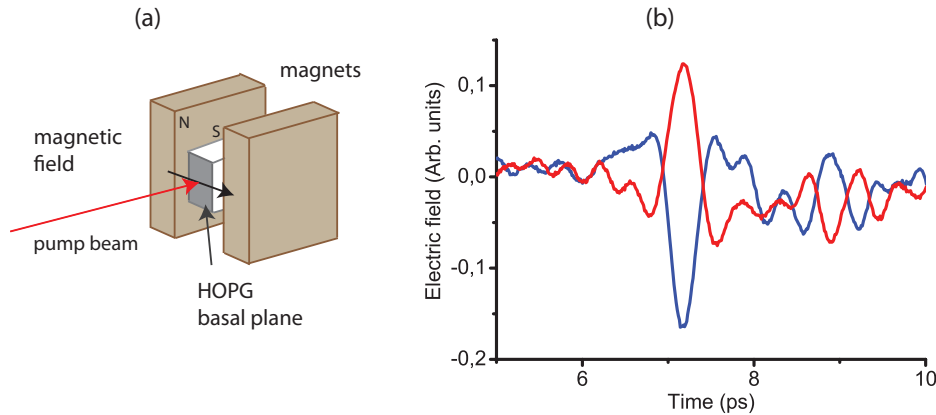
3.2 Magnetic-field enhancement

Fig. 3. (a) The schematic of the experimental setup used for applying in-plane magnetic-fields across the sample surface. (b) THz electric-field emitted from HOPG basal plane surface in the presence of in-plane magnetic-field; the blue and red traces indicate the two different cases with magnetic-fields of opposite sign.

Application of a magnetic field of about 1 T across the HOPG basal plane surface was found to affect the generated THz electric field amplitude and polarity. At 0° pump beam incidence, the THz radiation collected in the back-reflected direction is very weak, and is attributed to the imperfections of the crystal as mentioned earlier. When the magnetic-field is applied, in the plane parallel to the optical table and perpendicular to the c-axis of the crystal as shown in Fig. 3(a), we see an enhancement of the originally very weak, vertically polarized component of the emitted THz electric-field. Ideally, in this configuration, the THz electric-field is detected only in the presence of the magnetic-field. When the magnetic-field is reversed, the polarity of the THz pulse reverses too (Fig. 3(b)). This strongly suggests the creation of a magnetic-field induced current component in the vertical direction, parallel to the basal plane surface. In this picture, the illumination of the surface with femtosecond laser pulses initially causes a transient current along the c-axis, perpendicular to the surface. When illuminated at 0° angle of incidence, little or no THz emission is therefore observed in the back-reflected direction, as mentioned earlier. The application of the magnetic-field creates a Lorentz force acting on the moving charges, which adds a vertical in-plane component to the current, and thus creates a vertically polarized THz electric-field component [15–18].

We note that historically, before the exact cause for the magnetic field-induced changes in THz emission for semiconductors was known, an enhancement factor was used to phenomenologically describe the magnetic-field induced changes in the emitted THz amplitude. For a perfect sample, when without magnetic field no THz radiation is emitted in the back-reflected direction, an infinitely large enhancement factor would result when a magnetic-field is applied. Here, when, presumably due to the polycrystalline nature of the sample, some THz light is emitted in the back-reflected direction, defining such an enhancement factor would not be very useful.

3.3 Edge-plane surface illumination

The edge plane surface contains the c-axis of the crystal. When the edge plane surface is illuminated, therefore, two configurations are possible; one with the c-axis in the plane of incidence and the other with the c-axis perpendicular to the plane of incidence. The generated THz radiation is always found to be polarized along the c-axis of the crystal at 0° illumination, similar to the earlier observation that there is a charge movement along the c-axis of the crystal. The THz pulse generated at 45° illumination is also polarized such that, a transient charge movement takes place along the c-axis. For both 0° and 45° illuminations, the THz electric fields emitted from the edge plane surface are strong and comparable in amplitude with the THz electric-field generated from the basal plane surface at 45° illumination.
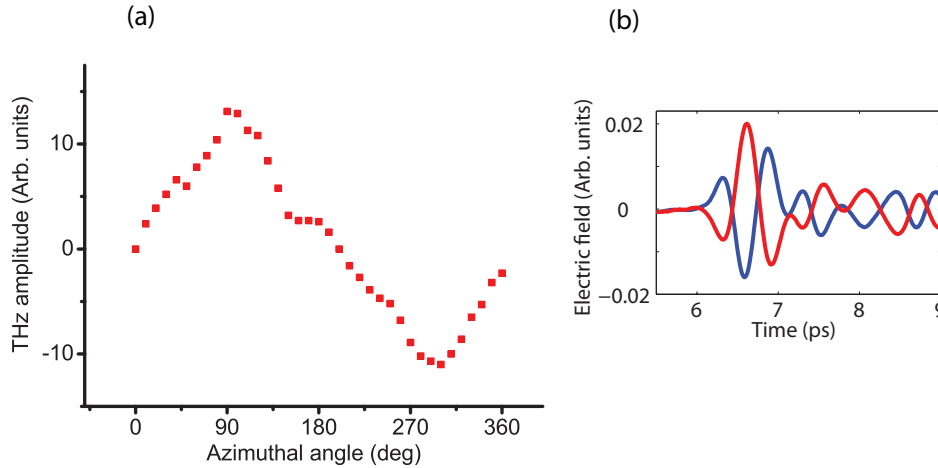
(a) (b)

Fig. 4. (a) The azimuthal angle dependence of the THz electric-field amplitude from the edge plane of the HOPG crystal. (b) The electric-field transients observed for the crystal azimuthal angles of 90° (red) and 270° (blue).

The azimuthal-angle dependence from the edge plane surface of the crystal for 45° angle of incidence illumination is shown in Fig. 4(a). When we rotate the crystal about the surface normal, the polarization of the emitted THz radiation rotates with it, always remaining in a plane perpendicular to the surface containing the c-axis. The figure shows the variation of the p-polarized component of the emitted THz electric-field for a complete azimuthal rotation of the crystal by 360°. The generated THz electric-field flips sign when the sample is rotated by 180° about the surface normal. In order to further illustrate this, two THz pulses emitted from the crystal oriented at 90° and 270° azimuthal angles are shown in Fig. 5(b). Note that the electro-optic detection system is polarization sensitive and only one polarization component of the generated THz is detected at a time [10]. Magnetic-field enhancement measurements could not be performed in this case. It was impossible to prepare very thin edge-plane samples owing to the flaky nature of HOPG. However, the azimuthal angle dependence shown in Fig. 5(a) already strongly indicates that the transient charge movement at the edge-plane takes place mainly parallel to the sample surface. This means that an in-plane magnetic-field perpendicular to the transient currents, would lead to a decrease in the emitted THz amplitude whereas no effect would be observed when the two are parallel.

Combining the observations from both 0° and 45° angle of incidence illumination, we see that the generated THz radiation from HOPG surfaces is always polarized along the c-axis of the crystal. As mentioned earlier, a possible underlying mechanism for the generation of THz radiation is a transient charge movement along the c-axis of the crystal. The conductivity of graphite along the c-axis is known to be at least three orders of magnitude smaller than the conductivity along the graphene planes [2–5]. A preferred charge movement along the c-axis, following an ultrafast excitation of graphite, has not been reported in literature to our knowledge.

The THz electric-field generated from any basal plane surface, always has the same polarity. Even when new basal plane surfaces are created by repeatedly cleaving the sample, the surfaces from both new samples that are formed, give rise to the emission of THz radiation with the same polarity. There are at least two possible generation mechanisms involving charge movement that can give rise to THz emission. Graphite basal plane surfaces are reported to have a space charge layer of a few nanometers thickness [19,20]. The femtosecond laser-created charge carriers, accelerated in this space charge layer, can emit pulses of THz radiation. Another possible mechanism is the photo-Dember effect [21]. If the electron and hole mobilities along the HOPG c-axis are different, this can give rise to the development of a time-dependent dipole along the c-axis, which emits a THz electric-field pulse. These mechanisms are similar to that reported earlier for semiconductor surfaces, such as GaAs [22].

The azimuthal-angle dependence of the THz electric-field generated from the edge plane surface resembles that of an in-plane biased semiconductor surface where the photo-generated charge carriers move preferentially in one direction along the surface and which therefore reverses direction when the sample is rotated by 180°. However, here, no external bias is applied to the HOPG sample. The above proposed mechanisms for the emission of THz radiation from the basal plane surfaces, namely, carrier acceleration in a space charge layer and the photo-Dember effect, cannot completely explain this. Although HOPG is the best available well-oriented system of graphite, it does not constitute a perfect crystal. HOPG is known to contain stacking faults [23]. Graphite mainly exists in hexagonal form, but the rhombohedral form can also exist together with the hexagonal structure [4]. Stacking faults in the crystal can act as breaks in the conduction paths along the c-axis direction, which can lead to accumulation of charges [24,25]. These accumulated charges can lead to built-in electric potentials in the crystal. Along the c-axis, graphite is known to behave electrically like a semiconductor [4]. Perhaps these built-in potentials in the crystal can give rise to charge acceleration in a preferred direction leading to the emission of THz pulses when the edge plane surface is irradiated with femtosecond laser pulses [26]. This seems to imply that weaker THz electric-field would be emitted from the edge-planes of a sample with fewer stacking faults.

3.4 THz generation from pencil lead

Interestingly, we find that other forms of graphite are also capable of emitting THz pulses, when illuminated with femtosecond laser pulses. In fact, even the graphite present in pencil lead emits THz pulses when illuminated with femtosecond pulses. In Fig. 5 we show the THz electric-field amplitude measured as a function of position along a line across a pencil drawing on paper, consisting of two stripes, as shown in the inset. For this experiment, the laser beam was focused to a 1 mm spot-size on the paper. From the figure it is clear that only the graphite emits THz radiation and not the paper. Pencil-lead contains graphite as a major component along with clay and other substances which define its hardness. Our results illustrate that pencil drawings on paper not only reflect/absorb THz radiation [27], but can also be used to generate measurable amounts of THz radiation.
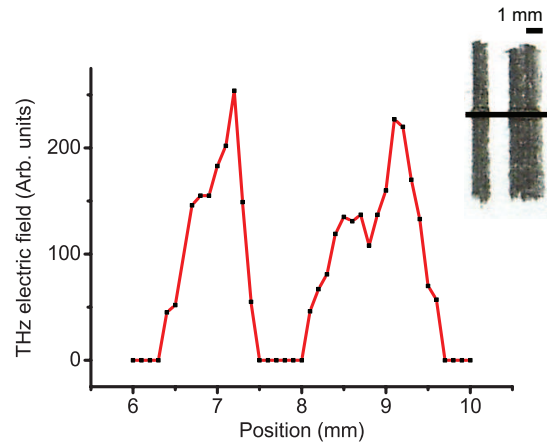
Fig. 5. The amplitude of the THz electric-field generated from a pencil drawing on paper as a function of position along a line shown in the inset. Inset: Photograph of the drawing.

4. Conclusion

In conclusion, we report the observation of the emission of transient subpicoseond pulses of electromagnetic radiation in the THz region, when graphite surfaces are illuminated with femtosecond laser pulses. The emitted THz radiation is mainly polarized along the c-axis of the crystal. The THz pulses emerging from the basal plane surface are most likely created by transient charge movement along the c-axis either because of the charge acceleration in the thin surface space charge layer of graphite, or because of the photo-Dember effect. Involvement of the charge carrier movement is confirmed by magnetic-field induced enhancements of the emitted THz electric-field. The emission of the THz pulses from the edge plane surfaces is tentatively ascribed to built-in potentials created by stacking faults in the material.

Acknowledgements